Towards the Fundamental Quantum Limit of Linear Measurements of Classical Signals

Haixing Miao, Rana X Adhikari, Yiqiu Ma, Belinda Pang, and Yanbei Chen

Phys. Rev. Lett. **119**, 050801 — Published 2 August 2017

DOI: 10.1103/PhysRevLett.119.050801

Towards the Fundamental Quantum Limit of Linear Measurements of Classical Signals

Haixing Miao,[1] Rana X Adhikari,[2] Yiqiu Ma,[3] Belinda Pang,[3] and Yanbei Chen[3]

[1]*School of Physics and Astronomy, Institute of Gravitational Wave Astronomy, University of Birmingham, Birmingham, B15 2TT, United Kingdom*
[2]*LIGO Laboratory, California Institute of Technology, Pasadena, CA 91125, USA*
[3]*Theoretical Astrophysics 350-17, California Institute of Technology, Pasadena, CA 91125, USA*

The quantum Cramér-Rao bound (QCRB) sets a fundamental limit for the measurement of classical signals with detectors operating in the quantum regime. Using linear-response theory and the Heisenberg uncertainty relation, we derive a general condition for achieving such a fundamental limit. When applied to classical displacement measurements with a test mass, this condition leads to an explicit connection between the QCRB and the Standard Quantum Limit which arises from a tradeoff between the measurement imprecision and quantum backaction; the QCRB can be viewed as an outcome of a quantum non-demolition measurement with the backaction evaded. Additionally, we show that the test mass is more a resource for improving measurement sensitivity than a victim of the quantum backaction, which suggests a new approach to enhancing the sensitivity of a broad class of sensors. We illustrate these points with laser interferometric gravitational wave detectors.

Introduction.— In high-precision measurements of classical signals, one challenge is to reduce various noise sources so that we can measure the tiny change in the detector state caused by the signal. This is often achieved by minimizing the coupling of the detector to the environment. Eventually, we approach the quantum regime with the dominant noise coming from the statistical nature of the detector quantum state. Maximizing the quantum-limited sensitivity requires proper preparation of the detector state and measurements of its observables—a key task in quantum metrology (cf. the review article by Giovannetti *et al.* [1]). The quantum Cramér-Rao bound (QCRB), derived in the pioneering works of Helstrom [2] and Holevo [3], sets a fundamental limit to the maximum sensitivity for a given detector state. As proved by Braunstein *et al.* [4, 5], this lower bound can be attained only if (i) the detector state is pure and the right observable is measured, so that the quantum Fisher information becomes equal to its classical counterpart, and (ii) the estimator based upon the measurement records is efficient, i.e., the mean squared estimation error saturates the classical Cramér-Rao bound.

In linear measurements, as illustrated in Fig. 1, the detector input port observable, $\hat{F}$, is linearly coupled to the signal, x. In the case of single-shot detection of a single-parameter signal, this is modelled by the interaction $\hat{H}_{\rm int} = -\hat{F}\,x\,\delta(t)$, and the QCRB for the estimation error, σ_{xx}, is (cf., Chapter 2 of Ref. [6])

$$\sigma_{xx}^{\rm QCRB} = \frac{\hbar^2}{4\langle\psi|\hat{F}^2|\psi\rangle}\,, \tag{1}$$

where $|\psi\rangle$ is the initial detector state, and we assume that $\langle\psi|\hat{F}|\psi\rangle = 0$. To attain it, the output-port observable, $\hat{Z}$, that we measure needs to satisfy [4],

$$\mathrm{Re}[\langle\psi|\hat{\Pi}_z\,\hat{F}|\psi\rangle] = 0 \quad \forall z\,, \tag{2}$$

where $\mathrm{Re}[\cdot]$ means taking the real part, and the projection operator $\hat{\Pi}_z$ is defined as $\hat{\Pi}_z \equiv |z\rangle\langle z|$ with $|z\rangle$ being an eigenstate of $\hat{Z}$ and z the measurement outcome. The maximum-likelihood estimator of x, based upon z, will be efficient if $|\psi\rangle$ is Gaussian, or the sample size is large [7].

For detecting signals with multi-dimensional parameters, the QCRB is not as simple [8] as the one shown in Eq. (1). In particular, Tsang *et al.* [9] generalized the QCRB to the linear measurement of a continuous signal $x(t)$ with an infinite-dimensional parameter space (specifically gravitational wave detection using laser interferometers [10, 11]). For time-invariant, linear detectors with $\hat{H}_{\rm int} = -\hat{F}\,x(t)$, they showed that the QCRB for estimating the Fourier components, $x(\omega)$, of the signal is

$$\sigma_{xx}^{\rm QCRB}(\omega) = \frac{\hbar^2}{4\bar{S}_{FF}(\omega)}\,, \tag{3}$$

where $\bar{S}_{FF}$ is the symmetrized power spectral density that describes the quantum fluctuations (uncertainty) of $\hat{F}$. Braginsky *et al.* [12] also derived a similar result, in terms of the signal-to-noise ratio.

Until now, it has not been shown generally how the QCRB in Eq. (3) can be achieved. This is, however, crucial for applying the QCRB to guide the design of quantum-limited linear sensors. We fill this gap by showing general conditions for achieving the bound: (1) the detector is at the quantum limit with minimum uncertainty, and (2) the observables $\hat{Z}$ and $\hat{F}$ are uncorrelated (in terms of cross-spectrum):

$$\bar{S}_{ZF}(\omega) = 0\,. \tag{4}$$

One can find the optimal $\hat{Z}$ satisfying the second condition if the imaginary part of the input susceptibility χ_{FF} vanishes:

$$\mathrm{Im}[\chi_{FF}(\omega)] = 0\,. \tag{5}$$

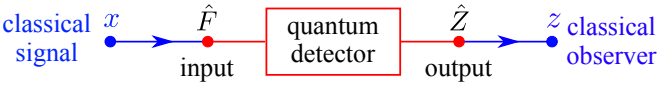

FIG. 1. (color online) A schematic for a quantum measurement of a classical signal using a linear detector. One degree of freedom of the detector is singled out as the input port, for which the observable, $\hat{F}$, is coupled to the signal, x, and another one as the output port with its observable, $\hat{Z}$, projectively measured by the observer. The detector is a quantum interface between two classical domains.

When this is not the case and we only have the first condition satisfied, the minimal estimation error will still be bounded:

$$\sigma_{xx}^{\mathrm{QCRB}} \le \min \sigma_{xx} \le 2\,\sigma_{xx}^{\mathrm{QCRB}}. \tag{6}$$

In deriving the above results, we use the linear-response theory developed by Kubo [13], which has previously been applied to analyze the quantum limited sensitivity of linear detectors [14–17]. Additionally, we apply the recent result on the Heisenberg uncertainty relation for continuous quantum measurements presented in Ref. [18].

Single-shot Measurements.— Before discussing the continuous measurements, we will first illustrate the basic formalism using the example of a single-shot measurement with $\hat{H}_{\mathrm{int}} = -\hat{F}\,x\,\delta(t)$. Such an interaction will leave $\hat{F}$ unchanged, but induce a shift on any observable that does not commute with $\hat{F}$. Specifically, the solution to $\hat{Z}$ reads

$$\hat{Z} = \hat{Z}^{(0)} + (i/\hbar)[\hat{Z}^{(0)},\, \hat{F}^{(0)}]\,x \tag{7}$$

where the superscript (0) denotes evolution under the detector free Hamiltonian $\hat{H}_{\mathrm{det}}$. For linear detectors, the canonical coordinates have classical-number (i.e., not operator) commutators, and $\hat{H}_{\mathrm{det}}$ only contains their linear or quadratic functions. The relevant observables, $\hat{Z}$ and $\hat{F}$, also depend linearly on the canonical coordinates. This justifies application of linear-response theory, in which different quantities are linked by classical-number susceptibilities. A brief introduction to the linear-response theory is in the supplemental material.

In this example, we introduce the following susceptibility:

$$\chi_{ZF} \equiv (i/\hbar)[\hat{Z}^{(0)},\, \hat{F}^{(0)}]\,, \tag{8}$$

which quantifies response of the detector output to the signal: $\hat{Z} = \hat{Z}^{(0)} + \chi_{ZF}\,x$. Given the projective measurement of $\hat{Z}$, we can construct an unbiased estimator of the signal:

$$\hat{x}_{\mathrm{est}} = \hat{Z}/\chi_{ZF}\,. \tag{9}$$

The resulting mean squared error σ_{xx} is determined by the quantum uncertainty of $\hat{Z}^{(0)}$, i.e.,

$$\sigma_{xx} \equiv \mathrm{Tr}[\hat{\rho}_{\mathrm{det}}(\hat{x}_{\mathrm{est}} - x)^2] = \sigma_{ZZ}/\chi_{ZF}^2\,, \tag{10}$$

where $\sigma_{ZZ} \equiv \mathrm{Tr}[\hat{\rho}_{\mathrm{det}}(\hat{Z}^{(0)})^2]$ assuming zero mean and $\hat{\rho}_{\mathrm{det}}$ is the density matrix of the detector initial state. From the general Heisenberg uncertainty relation between $\hat{Z}^{(0)}$ and $\hat{F}^{(0)}$:

$$\sigma_{ZZ}\sigma_{FF} - \sigma_{ZF}^2 \ge (\hbar^2/4)\chi_{ZF}^2 \tag{11}$$

with $\sigma_{ZF} \equiv \mathrm{Tr}[\hat{\rho}_{\mathrm{det}}(\hat{Z}^{(0)}\hat{F}^{(0)} + \hat{F}^{(0)}\hat{Z}^{(0)})/2]$ being their cross correlation, we obtain

$$\sigma_{xx} \ge \frac{\hbar^2}{4\sigma_{FF}} + \frac{\sigma_{ZF}^2}{\sigma_{FF}\chi_{ZF}^2} \ge \frac{\hbar^2}{4\sigma_{FF}} = \sigma_{xx}^{\mathrm{QCRB}}\,. \tag{12}$$

Achieving the QCRB therefore requires that the detector is at quantum limit with minimum uncertainty, i.e., in a pure Gaussian state with Eq. (11) taking the equal sign, and additionally

$$\sigma_{ZF} = 0\,. \tag{13}$$

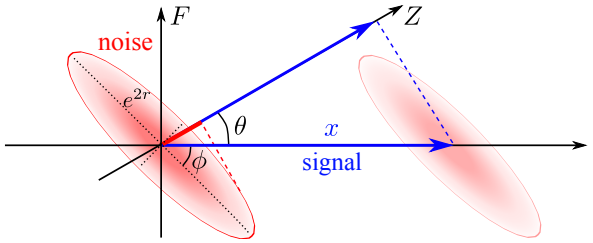

FIG. 2. (color online) Illustration of the single-shot measurement with the detector in a pure, Gaussian, squeezed state (the noise ellipse represents its Wigner function). The optimal observable $\hat{Z}$ to achieve the QCRB is neither the conjugate variable of $\hat{F}$ (along the horizontal axis), which contains the largest signal, nor the one having the minimum noise (parallel to the semi-minor axis of the noise ellipse). Instead it is the one uncorrelated with $\hat{F}$ and $\tan\theta = \sin(2\phi)\sinh(2r)/[\cosh(2r) + \cos(2\phi)\sinh(2r)]$, in which r and ϕ are the squeezing factor and angle, as derived in Ref. [5] using Eq. (2).

Since $\hat{Z} = \int \mathrm{d}z\,\hat{\Pi}_z\,z$, this condition is equivalent to Eq. (2). When discussing a similar example, Braunstein *et al.* [5] derived the optimal $\hat{Z}$ using Eq. (2), as illustrated in Fig. 2.

Continuous Measurements.— The discussion for the continuous measurements is quite similar to the single-shot case, but with additional complications due to the involvement of many degrees of freedom—the detector is a continuum field. We focus on linear detectors that are time-invariant, i.e., having a time-independent $\hat{H}_{\mathrm{det}}$ and being in a stationary state $[\hat{\rho}_{\mathrm{det}}, \hat{H}_{\mathrm{det}}] = 0$, allowing for frequency-domain analysis of both dynamics and noise.

As in Eq. (7), $\hat{Z}$ in the continuous case is given by

$$\hat{Z}(t) = \hat{Z}^{(0)}(t) + \int_{-\infty}^{\infty} \mathrm{d}t'\chi_{ZF}(t-t')\,x(t') \tag{14}$$

with the susceptibility, $\chi_{ZF} \equiv (i/\hbar)[\hat{Z}^{(0)}(t),\, \hat{F}^{(0)}(t')]\Theta(t-t')$, a function of the time difference $t-t'$. In the frequency domain, it becomes

$$\hat{Z}(\omega) = \hat{Z}^{(0)}(\omega) + \chi_{ZF}(\omega)x(\omega)\,, \tag{15}$$

where $f(\omega) \equiv \int_{-\infty}^{+\infty} \mathrm{d}t\, e^{i\omega t} f(t)$. The unbiased estimator of $x(\omega)$, following Eq. (9), is then $\hat{x}_{\mathrm{est}}(\omega) = \hat{Z}(\omega)/\chi_{ZF}(\omega)$.

Given that the detector is in a stationary state, the quantum fluctuation can be quantified by using the spectral density. There is also a Heisenberg uncertainty relation for the continuous measurements in terms of spectral densities and susceptibilities (cf., Chapter VI in Ref. [16] or Ref. [18]):

$$\bar{S}_{ZZ}(\omega)\bar{S}_{FF}(\omega) - |\bar{S}_{ZF}(\omega)|^2 \ge \frac{\hbar^2}{4}|\chi_{ZF}(\omega)|^2 + \hbar\left|\mathrm{Im}[\bar{S}_{ZZ}(\omega)\chi_{FF}(\omega) - \bar{S}_{ZF}^*(\omega)\chi_{ZF}(\omega)]\right|\,. \tag{16}$$

Here the symmetrized spectral densities $\bar{S}_{ZZ}$, $\bar{S}_{FF}$ and $\bar{S}_{ZF}$ are defined as $\bar{S}_{AB}(\omega) \equiv [S_{AB}(\omega) + S_{BA}(-\omega)]/2$ with the unsymmetrized one S_{AB} defined by $\mathrm{Tr}[\hat{\rho}_{\mathrm{det}}\,\hat{A}^{(0)}(\omega)\hat{B}^{(0)\dagger}(\omega')] \equiv 2\pi\,S_{AB}(\omega)\delta(\omega-\omega')$ [17]; χ_{FF} is defined in the same way as χ_{ZF} in Eq. (14) and with $\hat{Z}^{(0)}$ replaced by $\hat{F}^{(0)}$.

With Eq. (16), the error $\sigma_{xx}(\omega) \equiv \bar{S}_{ZZ}(\omega)/|\chi_{ZF}(\omega)|^2$ for estimating $x(\omega)$ thus satisfies

$$\sigma_{xx}(\omega) \geq \frac{\hbar^2}{4\bar{S}_{FF}} + \frac{|\bar{S}_{ZF}|^2 + \hbar|\mathrm{Im}[\bar{S}_{ZZ}\chi_{FF} - \bar{S}^*_{ZF}\chi_{ZF}]|}{\bar{S}_{FF}|\chi_{ZF}|^2} . \quad (17)$$

As proven in Ref. [18], when the detector is at the quantum limit, i.e., in a pure, stationary, Gaussian state—the multimode squeezed state [19], not only does Eq. (16) become an equality, but also we have

$$\mathrm{Im}[\bar{S}_{ZZ}(\omega)\chi_{FF}(\omega) - \bar{S}^*_{ZF}(\omega)\chi_{ZF}(\omega)]|_{\text{quantum limit}} = 0 . \quad (18)$$

At this point, we only require Eq. (4) to attain the QCRB—the first term in Eq. (17).

We now show that if Eq. (5) is satisfied, the optimal observable $\hat{Z}$, which realizes Eq. (4), exists. In general, $\hat{Z}$ is a linear combination of two conjugate variables (denoted by $\hat{Z}_{1,2}$) of the output port, up to some constant:

$$\hat{Z}(\omega) = \hat{Z}_1(\omega)\sin\theta + \hat{Z}_2(\omega)\cos\theta . \quad (19)$$

Eq. (4) can then be realized if there is a real solution to θ:

$$\tan\theta = -\bar{S}_{Z_2F}(\omega)/\bar{S}_{Z_1F}(\omega) \in \text{Reals}, \quad (20)$$

or $\mathrm{Im}[\bar{S}_{Z_1F}(\omega)\bar{S}^*_{Z_2F}(\omega)] = 0$. This turns out to be equivalent to $\mathrm{Im}[\chi_{FF}(\omega)] = 0$ due to the following equality:

$$\mathrm{Im}[\bar{S}_{Z_1F}(\omega)\bar{S}^*_{Z_2F}(\omega)] = (\hbar/4)\mathrm{Im}[\chi_{FF}(\omega)] , \quad (21)$$

which is generally valid for detectors at the quantum limit.

If $\mathrm{Im}[\chi_{FF}]$ is nonzero, we will not find the optimal $\hat{Z}$ that exactly achieves the QCRB. Nevertheless, the estimation error σ_{xx}, minimized over all possible θ in Eq. (19), is still bounded as shown in Eq. (6). This is because

$$\min_\theta \left|\bar{S}_{ZF}(\omega)/\chi_{ZF}(\omega)\right| \leq \hbar/2 . \quad (22)$$

Including Eq. (17), the above inequality implies Eq. (6). The detailed proofs for Eqs. (21) and (22) are provided in the supplemental material [20].

Classical Displacement Measurements.— The above discussion applies to general linear measurements. Here we specifically look measurements of displacement; the detector often consists of a quantum field and a test mass with its position being displaced by a classical signal, which can be a result of the action of a force signal. The interaction between the field and the test mass leads to an important sensitivity limit—the Standard Quantum Limit (SQL), first derived by Braginsky [16]. Below we show an explicit connection between the SQL and the QCRB, and also discuss the active role of the test mass in enhancing the detector sensitivity.

In terms of a mathematical description, we denote the input port observable of the field as $\hat{\mathcal{F}}$ and the output as $\hat{\mathcal{Z}}$, to distinguish from $\hat{F}$ and $\hat{Z}$ (relevant for the entire detector); $\hat{\mathcal{F}}$ is coupled to the test mass position $\hat{q}$ via the interaction $-\hat{q}\hat{\mathcal{F}}$, and $\hat{\mathcal{Z}}$ is projectively measured. Solving the detector dynamics leads to (in the frequency domain):

$$\hat{F}^{(0)} = \frac{\hat{\mathcal{F}}^{(0)}}{1-\chi_{qq}\chi_{\mathcal{F}\mathcal{F}}} , \quad \hat{Z}^{(0)} = \hat{\mathcal{Z}}^{(0)} + \frac{\chi_{\mathcal{Z}\mathcal{F}}\chi_{qq}\hat{\mathcal{F}}^{(0)}}{1-\chi_{qq}\chi_{\mathcal{F}\mathcal{F}}} . \quad (23)$$

In the literature, the first term $\hat{\mathcal{Z}}^{(0)}$ of the detector output observable $\hat{Z}^{(0)}$ is referred to as the imprecision noise; the second term, proportional to $\hat{\mathcal{F}}^{(0)}$, is the quantum backaction noise.

For the special case when the input susceptibility of the field is zero: $\chi_{\mathcal{F}\mathcal{F}} = 0$, the resulting estimation error is

$$\sigma_{xx} = \frac{\bar{S}_{\mathcal{Z}\mathcal{Z}}}{|\chi_{\mathcal{Z}\mathcal{F}}|^2} + 2\mathrm{Re}\left[\chi^*_{qq}\frac{\bar{S}_{\mathcal{Z}\mathcal{F}}}{\chi_{\mathcal{Z}\mathcal{F}}}\right] + |\chi_{qq}|^2\bar{S}_{\mathcal{F}\mathcal{F}} . \quad (24)$$

If the imprecision noise and the backaction noise are uncorrelated, i.e. $\bar{S}_{\mathcal{Z}\mathcal{F}} = 0$, its lower bound will be the SQL:

$$\sigma_{xx} = \frac{\bar{S}_{\mathcal{Z}\mathcal{Z}}}{|\chi_{\mathcal{Z}\mathcal{F}}|^2} + |\chi_{qq}|^2\bar{S}_{\mathcal{F}\mathcal{F}} \geq \hbar|\chi_{qq}| \equiv \sigma^{\mathrm{SQL}}_{xx} . \quad (25)$$

The SQL can be surpassed by using quantum non-demolition (QND) measurements [21]: e.g., coherent noise cancellation schemes [22] or equivalently, optimal readout schemes [23] which cancel the backaction noise. In particular, optimal readout schemes utilize quantum correlations $\bar{S}_{\mathcal{Z}\mathcal{F}}$, and can be understood by applying the uncertainty relation $\bar{S}_{\mathcal{Z}\mathcal{Z}}\bar{S}_{\mathcal{F}\mathcal{F}} \geq |\bar{S}_{\mathcal{Z}\mathcal{F}}|^2 + \hbar^2|\chi_{\mathcal{Z}\mathcal{F}}|^2/4$ to rewrite Eq. (24) as

$$\sigma_{xx} \geq \frac{\hbar^2}{4\bar{S}_{\mathcal{F}\mathcal{F}}} + \left|\frac{\bar{S}_{\mathcal{Z}\mathcal{F}}}{\chi_{\mathcal{Z}\mathcal{F}}} + \chi_{qq}\bar{S}_{\mathcal{F}\mathcal{F}}\right|^2 \geq \frac{\hbar^2}{4\bar{S}_{\mathcal{F}\mathcal{F}}} . \quad (26)$$

The ultimate bound will be the QCRB if we read out the optimal output observable satisfying $\bar{S}_{\mathcal{Z}\mathcal{F}}/\chi_{\mathcal{Z}\mathcal{F}} + \chi_{qq}\bar{S}_{\mathcal{F}\mathcal{F}} = 0$, which, from Eq. (23), is equivalent to Eq. (4) shown earlier. The SQL can therefore be viewed as arising from a suboptimal readout scheme.

In cases where $\chi_{\mathcal{F}\mathcal{F}}$ is not zero, one can similarly show that the estimation error is again bounded by the QCRB:

$$\sigma_{xx} \geq \frac{\hbar^2}{4\bar{S}_{FF}} = \frac{\hbar^2}{4\bar{S}_{\mathcal{F}\mathcal{F}}}|1-\chi_{qq}\chi_{\mathcal{F}\mathcal{F}}|^2 . \quad (27)$$

In contrast to Eq. (26), here we have a factor of $|1-\chi_{qq}\chi_{\mathcal{F}\mathcal{F}}|^2$, which can be smaller than unity. There are two equivalent interpretations: (1) the test mass response is modified by the quantum field:

$$\chi^{\mathrm{eff}}_{qq} = \frac{\chi_{qq}}{1-\chi_{qq}\chi_{\mathcal{F}\mathcal{F}}} ; \quad (28)$$

and (2) the quantum fluctuations of the field are modified by the test mass, as manifested by the relation between $\hat{F}^{(0)}$ and $\hat{\mathcal{F}}^{(0)}$ in Eq. (23). The latter highlights the active (and enhancing) role of the test mass, rather than being a victim of the quantum backaction. Below, we illustrate this using gravitational wave (GW) detection with laser interferometers as an example.

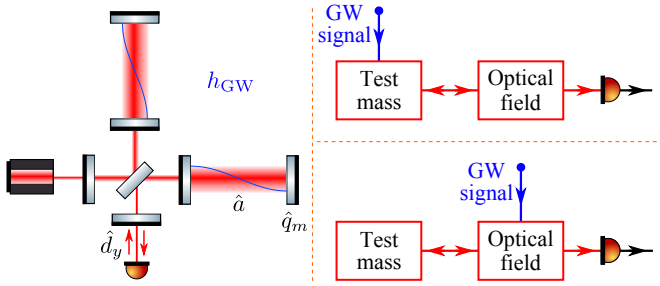

FIG. 3. (color online) Schematic diagram of a LIGO-like interferometer (left). Two approximately equivalent physical pictures for the detection principle (right).

Gravitational-wave Detection.— A typical GW detector, such as LIGO [24], is shown schematically in Fig. 3. This is an interferometer with Fabry-Pérot arm cavities formed by suspended mirrors (test masses). The usual picture of the detection principle envisions the GW as a tidal force on the test masses, and the resulting differential motion being probed by the optical field. Another picture is to view the GW as a strain directly coupled to the optical field [25, 26]. The latter is more appropriate when the GW wavelength is comparable to or shorter than the interferometer arm length, otherwise it is approximately equivalent to the former. We will apply it in later discussions to highlight the active role of the test mass mentioned earlier.

Putting the GW detection under the general framework, the classical signal is

$$x = L_{\rm arm} h_{\rm GW}\,, \tag{29}$$

where $L_{\rm arm}$ is the arm length, and $h_{\rm GW}$ is the GW strain. The test mass motion that we care about is the differential mode of the four mirrors in the two arms, with the susceptibility:

$$\chi_{qq} = -4/(M\,\omega^2)\,, \tag{30}$$

where M is the mirror mass. The quantum field is the optical field, coupled to the test mass via the radiation pressure.

As shown in Refs. [27, 28], the entire interferometer can be mapped to a single-cavity-mode optomechanical device, described by the standard cavity optomechanics [29]. The input observable $\hat{\mathcal{F}}$ is the time-varying part of the radiation pressure, which is proportional to the amplitude quadrature $\hat{X}$ of the cavity mode:

$$\hat{\mathcal{F}} = 2P_{\rm cav}/c = \hbar g \hat{X}\,, \tag{31}$$

of which the relevant susceptibility is given by [27]:

$$\chi_{\mathcal{F}\mathcal{F}} = \frac{\hbar g^2 \Delta}{(\omega - \Delta + i\gamma)(\omega + \Delta + i\gamma)}\,. \tag{32}$$

Here $g \equiv 2\sqrt{\bar{P}_{\rm cav}\omega_{\rm cav}/(\hbar L_{\rm arm} c)}$ with $\bar{P}_{\rm cav}$ the average optical power inside the cavity and $\omega_{\rm cav}$ the cavity resonant frequency; $\Delta = \omega_0 - \omega_{\rm cav}$ is the detuning of the laser frequency

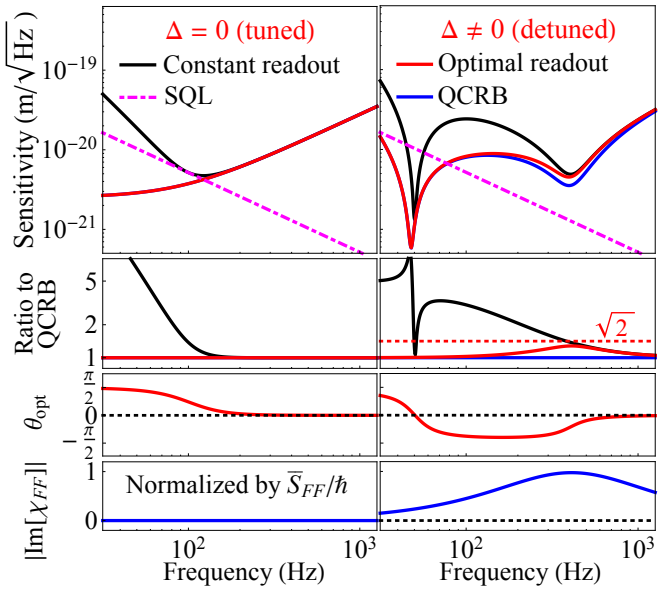

FIG. 4. (color online) The top row shows the QCRB (solid curve) for LIGO-type GW detector with detuning frequency $\Delta = 0$ (left) and $\Delta/(2\pi) = 400$ Hz (right), and various sensitivity curves for comparison: (i) dash curve—constant phase quadrature readout, (ii) dash-dot curve—readout quadrature optimized to maximize sensitivity at each frequency, and (iii) dot curve—the SQL $\sqrt{4\hbar/(M\omega^2)}$. The bottom row shows the ratio to the QCRB for selected curves. Other relevant parameters are: $M = 40$ kg, $P_{\rm cav} = 800$ kW, $L_{\rm arm} = 4$ km, $\gamma/(2\pi) \approx 100$ Hz, and laser frequency $\omega_0/(2\pi) \approx 3 \times 10^{14}$ Hz.

ω_0; γ is the cavity bandwidth. The output observable $\hat{\mathcal{Z}}$ is a linear combination of the amplitude and phase quadrature of the outgoing field at the dark (differential) port.

In Fig. 4, we plot the resulting QCRB for the two cases: $\Delta = 0$ (tuned) and $\Delta \neq 0$ (detuned), assuming other parameters similar to LIGO. In comparison, we have also included the SQL, and the estimation error $\sigma_{xx}^{1/2}$, i.e. the sensitivity, for the phase quadrature readout and the optimal readout. The tuned case having $\chi_{\mathcal{F}\mathcal{F}} = 0$ provides a concrete example of Eq. (25) and Eq. (26). Indeed, the optimal readout, which surpasses the SQL by canceling the backaction noise, leads to a sensitivity exactly equal to the QCRB.

In the detuned case with $\chi_{\mathcal{F}\mathcal{F}} \neq 0$, the first point we want to highlight is that the maximum difference between the optimal-readout sensitivity, considered by Harms *et al.* [30], and the QCRB is at most $\sqrt{2}$ in amplitude, in accordance with our general result Eq. (6). The second point is that there are two noticeable dips in the QCRB. They imply that the amplitude quadrature of the cavity mode has higher fluctuations around these dips than other frequencies. Both can be interpreted as arising from positive feedback induced optical resonance. The higher frequency one coincides with the detuning frequency, which is at the cavity resonance. The low frequency one provides an example of the extra factor $|1 - \chi_{qq}\chi_{\mathcal{F}\mathcal{F}}|^2$ in Eq. (27). Physically, this has to do with the ponderomotive squeezing (or amplification) effect [23, 31], which recently has been

demonstrated experimentally [32–34]. The test mass acts as a Kerr-type nonlinear medium converting the amplitude fluctuations into the phase fluctuations, which in turn, feeds back to the amplitude quadrature due to the cavity detuning. Since the test mass susceptibility goes as $1/\omega^2$, cf. Eq. (30), the feedback gain is frequency dependent, resulting in the sharp resonance feature. The underlying physics is similar to the intracavity squeezing studied theoretically by Peano *et al.* [35] and experimentally by Korobko *et al.* [36].

An equivalent interpretation of the low frequency dip was presented in Refs. [27, 37]. It was attributed to the so-called optical spring effect, an example of Eq. (28)—the optomechanical interaction changes the test mass dynamics by creating a new mechanical resonance, around which the response to GWs is enhanced. The previous optical feedback interpretation, however, removes the distinction between optics and mechanics—the role of the latter also modifies the quantum fluctuations of the optical field. This suggests a new approach to designing optomechanical sensors. We can add proper optical filters in the feedback loop, together with the internal ponderomotive squeezing, to shape the optical feedback gain, so that the quantum fluctuation of the field is enhanced in the frequency band of interest. Since the sensitivity using the optimal readout is bounded, cf. Eq. (6), this will result in high detector sensitivity at relevant frequencies, with limitations only coming from the losses. Incorporating the effect of losses is critical and the subject of future work.

Acknowledgements.— We would like to thank members of the LSC MQM, AIC, and QN groups for fruitful discussions. HM is supported by UK STFC Ernest Rutherford Fellowship (Grant No. ST/M005844/11). RXA is supported by NSF grant PHY-0757058. YM, BP, and YC are supported by NSF PHY-0555406, PHY-0653653, PHY-0601459, PHY-0956189, PHY-1068881, as well as the David and Barbara Groce startup fund at Caltech. RXA, BP, and YC gratefully acknowledge funding provided by the Institute for Quantum Information and Matter, an NSF Physics Frontier Center with support of the Gordon and Betty Moore Foundation.

[1] V. Giovannetti, S. Lloyd, and L. Maccone, Nature Photonics **5**, 222 (2011).
[2] C. Helstrom, Phys. Lett. A **25**, 101 (1967).
[3] A. Holevo, *Probabilistic and Statistical Aspects of quantum theory*, 2nd ed. (Scuola Normale Superiore, 2011).
[4] S. L. Braunstein and C. M. Caves, Phys. Rev. Lett. **72**, 3439 (1994).
[5] S. L. Braunstein, C. M. Caves, and G. J. Milburn, Annals of Physics **247**, 135 (1996).
[6] H. M. Wiseman and G. J. Milburn, *Quantum Measurement and Control* (Cambridge University Press, 2010).
[7] Due to the central limit theorem. In this case, an extra factor of $1/N$ (N the sample size) shall be included in the bound above.
[8] M. Szczykulska, T. Baumgratz, and A. Datta, Advances in Physics: X **1**, 621 (2016).
[9] M. Tsang, H. M. Wiseman, and C. M. Caves, Phys. Rev. Lett. **106**, 090401 (2011).
[10] C. M. Caves, Phys. Rev. D **23**, 1693 (1981).
[11] R. X. Adhikari, Rev. Mod. Phys. **86**, 121 (2014).
[12] V. B. Braginsky, M. L. Gorodetsky, F. Y. Khalili, and K. S. Thorne, AIP Conf. Proc. **523**, 180 (2000).
[13] R. Kubo, Reports on Progress in Physics **29**, 255 (1966).
[14] D. V. Averin, arXiv:cond-mat/0301524 (2003).
[15] A. A. Clerk, S. M. Girvin, and A. D. Stone, Phys. Rev. B **67**, 165324 (2003).
[16] V. B. Braginsky and F. Khalilli, *Quantum Measurement* (Cambridge University Press, 1992).
[17] A. A. Clerk, M. H. Devoret, S. M. Girvin, F. Marquardt, and R. J. Schoelkopf, Rev. Mod. Phys. **82**, 1155 (2010).
[18] H. Miao, Phys. Rev. A **95**, 012103 (2017).
[19] K. J. Blow, R. Loudon, S. J. D. Phoenix, and T. J. Shepherd, Phys. Rev. A **42**, 4102 (1990).
[20] In addition to Refs. [13, 16, 17, 19, 37] mentioned in the main text, the supplemental material also includes Ref. [38].
[21] V. B. Braginsky and F. Y. Khalili, Reviews of Modern Physics **68**, 1 (1996).
[22] M. Tsang and C. M. Caves, Phys. Rev. Lett. **105**, 123601 (2010).
[23] H. J. Kimble, Y. Levin, A. B. Matsko, K. S. Thorne, and S. P. Vyatchanin, Phys. Rev. D **65**, 022002 (2001).
[24] LIGO Scientific Collaboration, Classical and Quantum Gravity **32**, 74001 (2015).
[25] F. I. Cooperstock and V. Faraoni, Classical and Quantum Gravity **10**, 1189 (1993).
[26] S. P. Tarabrin and A. A. Seleznyov, Phys. Rev. D **78**, 062001 (2008).
[27] A. Buonanno and Y. Chen, Phys. Rev. D **67**, 062002 (2003).
[28] Y. Chen, Journal of Physics B: Atomic, Molecular and Optical Physics **46**, 104001 (2013).
[29] M. Aspelmeyer, T. J. Kippenberg, and F. Marquardt, Rev. Mod. Phys. **86**, 1391 (2014).
[30] J. Harms, Y. Chen, S. Chelkowski, A. Franzen, H. Vahlbruch, K. Danzmann, and R. Schnabel, Phys. Rev. D **68**, 042001 (2003).
[31] T. Corbitt, Y. Chen, F. Khalili, D. Ottaway, S. Vyatchanin, S. Whitcomb, and N. Mavalvala, Phys. Rev. A **73**, 023801 (2006).
[32] D. W. C. Brooks, T. Botter, S. Schreppler, T. P. Purdy, N. Brahms, and D. M. Stamper-Kurn, Nature **488**, 476 (2012).
[33] T. P. Purdy, P. L. Yu, R. W. Peterson, N. S. Kampel, and C. A. Regal, Phys. Rev. X **3**, 031012 (2013).
[34] A. H. Safavi-Naeini, S. Gröblacher, J. T. Hill, J. Chan, M. Aspelmeyer, and O. Painter, Nature **500**, 185 (2013).
[35] V. Peano, H. G. L. Schwefel, C. Marquardt, and F. Marquardt, Phys. Rev. Lett. **115**, 243603 (2015).
[36] M. Korobko, L. Kleybolte, S. Ast, H. Miao, Y. Chen, and R. Schnabel, Phys. Rev. Lett. **118**, 143601 (2017).
[37] A. Buonanno and Y. Chen, Phys. Rev. D **65**, 042001 (2002).
[38] C. W. Gardiner and M. J. Collett, Phys. Rev. A **31**, 3761 (1985).